An Improved Instrument for Real-Time Measurement of Blood Flow Velocity in Microvessels

Article *in* IEEE Transactions on Instrumentation and Measurement · January 2008

DOI: 10.1109/TIM.2007.907959 · Source: IEEE Xplore

6 authors, including:

Francesca Sapuppo
University of Catania
49 PUBLICATIONS **352** CITATIONS
SEE PROFILE

Maide Bucolo
University of Catania
158 PUBLICATIONS **1,173** CITATIONS
SEE PROFILE

Marcos Intaglietta
University of California, San Diego
459 PUBLICATIONS **17,578** CITATIONS
SEE PROFILE

Luigi Fortuna
University of Catania
587 PUBLICATIONS **8,372** CITATIONS
SEE PROFILE

An Improved Instrument for Real-Time Measurement of Blood Flow Velocity in Microvessels

Francesca Sapuppo, *Student Member, IEEE*, Maide Bucolo, *Member, IEEE*, Marcos Intaglietta, Paul C. Johnson, Luigi Fortuna, *Fellow, IEEE*, and Paolo Arena, *Senior Member, IEEE*

***Abstract*—A new approach for the measurement of red blood cell velocity at the level of microcirculation has been developed and characterized. The new real-time and automated measurement system is based on the dual-slit methodology, and blood flow information is extracted from images and transduced into two analog photometric signals and then processed using a hybrid analog–digital system that performs the cross correlation of the signals in real time. The characterization of the system consists of a calibration with a known velocity target, yielding to the hyperbolic calibration curve velocity versus delay and the determination of the velocity detectable range from 0.3 to 120 mm/s. A theoretical study of the measurement uncertainty and parametric studies were carried out to test the system robustness to changes of parameters and to determine the optimal configuration that is applicable to various experimental conditions. The system was further tested in *in vivo* experiments in the rat cremaster preparation in different types of vessels and flow velocities to verify the consistency of the results, as compared with those from conventional measuring systems. In addition, the dynamic behavior of the system and its response to changes in the measured velocity were studied through a continuous velocity record that was obtained during an experimental procedure.**

***Index Terms*—Cross correlation, dual-slit methodology, dynamic measurements, *in vivo* experimentation, microcirculation, red blood cells (RBCs).**

I. Introduction

THE DEVELOPMENT of automatic real-time methods to determine microvascular functional parameters, such as red blood cell (RBC) flow velocity, has been an active area of development in the microcirculation research field.

These methods find their application in the diagnostics of pathologies such as retinal abnormalities, hypertension, and cancer, which can be characterized through the analysis of microvascular conditions that involve either angiogenic phenomena or functional changes in microcirculation. Moreover, current experimental studies that are associated with the development of artificial blood [1], [2] require information on blood flow behavior and the development of an analytical framework with which the consequences of altering physical properties of the blood can be analyzed [3].

The first step for the modeling of such a complex environment consists of objective measurements of structural and functional parameters in microcirculation. Suitable experimental models such as the hamster window model or rat preparation provide a direct visual/optical access to the microcirculation *in vivo*, offering parts of the body where the skin is thin and extensible.

Automated measurement methods are desirable for obtaining this type of information since manual operator-based measurements are prone to operator errors, are time consuming, and are potentially nonobjective.

Various blood velocity measurement experimental techniques exist for the microcirculation environment.

The ultrasonic Doppler flowmeter can be applied to small blood vessels, but contrast agents have to be used to meet the spatial resolution requirements for microcirculation applications. Several studies about interaction of ultrasound contrast agents with microcirculation assess that they might interfere with the normal activity due to their interaction with microvessel lumen [4] and extra-cellular structures [5], thus causing disruption, displacement, separation of endothelial cells, or a phenomenon known as inertial cavitation, leading to bubble destruction [6]–[8].

An alternative technique that is suitable for microcirculation studies is the optical Doppler intravital velocimeter. It can be used in microcirculatory vessels of all sizes, but there are problems in measuring flow in capillaries with tissues having two or more layers of capillaries since the signal is obtained from deeper vessels, as well as the superficial one that is in view. However, this is not a problem with arterioles and venules. Other limitations are that low light levels, tissue movements, and electronic noise can lead to erroneous readings [9]. It is also important to consider that methods based on frequency analyses present sensitivity to any periodic physiological phenomena interfering with the experimental setup, such as blood flow fluctuation due to the heartbeat or respiration [10].

An improved technique based on the Doppler principle is the enhanced high-resolution laser Doppler imaging (EHR-LDI). It is based on the principle of light scattering and on the

Manuscript received May 30, 2005; revised May 17, 2007. This work was supported in part by the Italian "Ministero dell'Istruzione, dell'Università e della Ricerca" (MIUR) funded project for the Internationalization of the Ph.D. School in Electronics and Automation of the University of Catania, Catania, Italy, and in part by the U.S. Public Health Service (USPHS) under Bioengineering Research Partnership Grant R24-HL64395. The work of M. Intaglietta was supported by the USPHS under Grant R01-HL62354 and Grant R01-HL62318. The work of P. C. Johnson was supported by the USPHS under Grant R01-HL66318.

F. Sapuppo, M. Bucolo, L. Fortuna, and P. Arena are with the Dipartimento di Ingegneria Elettrica Elettronica e dei Sistemi, University of Catania, 95125 Catania, Italy (e-mail: fsapuppo@diees.unict.it; mbucolo@diees.unict.it; lfortuna@diees.unict.it; parena@diees.unict.it).

M. Intaglietta and P. C. Johnson are with the Department of Bioengineering, University of California, San Diego, La Jolla, CA 92093 USA (e-mail: mintagli@ucsd.edu; pjohnson@bioeng.ucsd.edu).

Color versions of one or more of the figures in this paper are available online at http://ieeexplore.ieee.org.

Digital Object Identifier 10.1109/TIM.2007.907959

spectral analysis of the scattered signal to extract velocity information [11].

The EHR-LDI measurement can be performed using fluorescent tracers in blood vessels with diameters in the range from 10 to 210 μm. The EHR-LDI measurements can be evaluated in two ways according to the vessel size: 1) as a measure of RBC velocity (hematocrit is assumed to be constant) when the vessel diameter is larger than the width of the laser beam in the focal plane (40 μm) [12] and 2) as a volumetric flow estimate when the total measurement area containing the moving RBCs is smaller than the laser beam and therefore can be known. The velocity measurement is not absolute, but relative RBC velocities over the period of measurement can be obtained [13], [14]. Using the Duplex model [13], it is also possible to monitor the temporal RBC velocity changes in a predefined site, such as in a single vessel in the EHR-LDI image.

Particle image velocimetry (PIV) is another technique to assess blood flow velocity profiles and has been extensively used in experimental fluid mechanics. A number of variations of the PIV methods, such as the 2-D cross-correlation method, particle-tracking method, and iterative correlation method, have been reported [14], [15]. These techniques have been used to measure flow in microvessels. They are based on the analysis of charge-coupled device (CCD) camera recorded images and require high-speed digital video systems. The processing of high-resolution images yielding to a satisfactory resolution for intravital microscopy and the outputting of the velocity information for each point in the vessels are computationally demanding.

By comparison with the aforementioned methods, the dual-slit methodology [16] is a practical online method for measuring the transit time of RBCs between two optical windows and obtaining blood flow velocity data with a spatial resolution, which is flexible and dependent on the optical characteristic of the microscopy system (global magnification) and on the optical slit sizes and separation. On one side, such methodology, when based on the optical acquisition system, suffers from a drawback, which is typical of optical methods. It thus can be applied on parts of the body that are suitable to microscopy setup and, therefore, on parts of the skin that are extensible, free from any optical interference (e.g., hair and skin conditions), and transparent to light. Also, overlapping of information interferes with velocity measurements, and therefore, the targeted part of the body needs to be thin to avoid microvessel multilayer, allowing measurements only on the surface vessels. On the other side, the microcirculation *in vivo* experimentation is based on animal preparations that fulfill such requirements, and it benefits from an extremely feasible setup based on standard microscopy or on any optic system that offers image magnification. The dual-slit methodology is based on the use of the cross-correlation function on photometric signals coming from the light intensity information associated to the blood flow in the microscopy image of the blood flow in microvessels, but it could actually be performed on any type of signal representing the passage of RBCs. The cross correlation can be implemented using either an analog solution or a digital [17] solution, as reported in Section II.

This paper reports a further development of this methodology and its implementation based on a new analog–digital approach, which allows the simultaneous acquisition and real-time processing of the optical signals by an optimized cross-correlation algorithm and the automatic detection of blood flow velocity. We provide a description of the signal processing algorithm and its implementation using new hybrid analog–digital techniques (using hardware–software tools), as well as the system calibration and characterization and *in vivo* experimental results, including the analysis of the dynamic response of the system to velocity changes.

II. Measurement Methodologies

This methodology is based on the use of two optical windows (slits) that are positioned on the microscopic image of the vessel on its centerline to record the light fluctuations that are produced on each window by the passage of RBCs flowing through the vessels [16], [17]. The separation between the windows causes the downstream signal to be delayed with respect to the upstream signal. The RBC velocity is given by the ratio of the window separation, which is a property of the optical system, and the delay between signals, which has to be measured. The cross-correlation technique is a practical method for measuring delay between noisy signals based on the computation of the cross-correlation function, which has a maximum at the most probable delay between the two signals.

In the dual-slit methodology, the optical windows can be implemented using analog optic sensors (e.g., photodiodes and photomultipliers) that are applied directly to the microscope-magnified image. These techniques yield two analog voltage signals that are proportional to the light intensity changes at the slits. The number, size (width w and height h), and distance (slit separation SS) of the slits can be varied [18], [19] to modify the spatial resolution of the system, the accuracy, and sensitiveness of the delay measurement. Fig. 1 shows the functioning scheme of the dual-slit methodology for *in vivo* experimentation on animal preparations.

A conventional approach for the implementation of the cross correlation uses hardware solutions to yield real-time signal processing. Examples of this implementation are the Hewlett Packard (HP) digital correlator (Model 3721A, Delta T Product, Tucson, AZ) and the velocity tracker (Mod-102 B, Vista, Inc., San Diego, CA). These devices process two analog channels, where the analog signals are digitized.

The HP digital cross correlator (no longer manufactured) provides as output a cross-correlation curve that is represented by a vector of 100 points displayed via a shift register. The maximum of the correlation curve is obtained using a peak detector that finds the time delay corresponding to the maximum correlation and gives an analog output voltage proportional to the velocity.

One of the drawbacks of this system is that the amplification applied to upstream and downstream signals affects the correlogram shape and amplitude and, therefore, the peak detection process. The velocity measurement will be considered consistent and correct only if the correlogram is clearly and completely displayed in the output window [Fig. 2(d)].

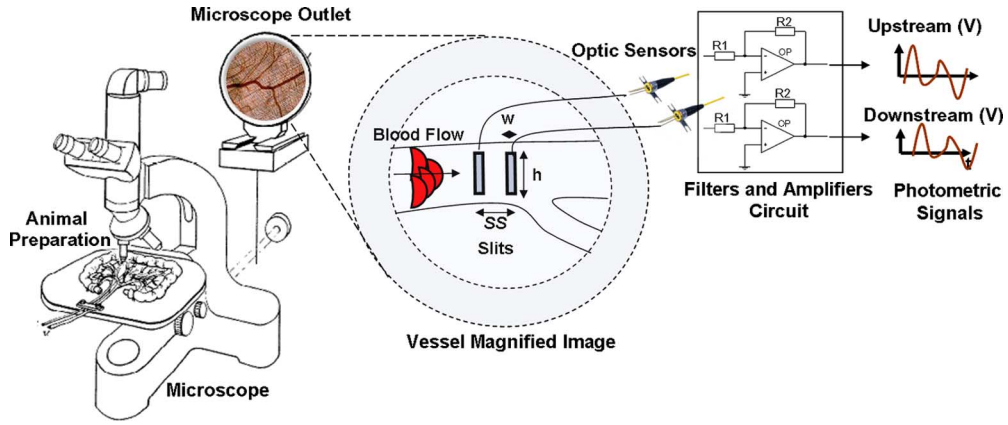

Fig. 1. Scheme of the dual-slit methodology implementation for *in vivo* experimentation on animal preparations.

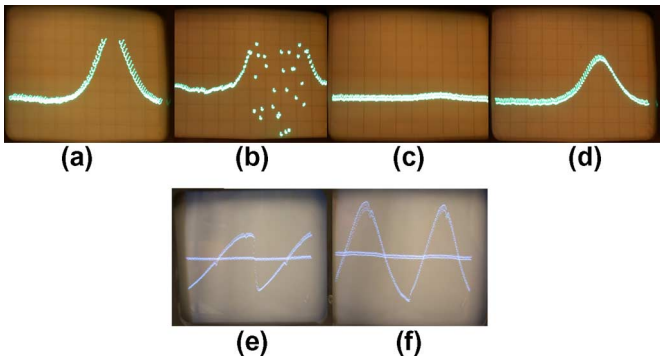

Fig. 2. HP digital correlator display window. (a) and (b) Saturation effects on the correlogram. (c) Flat correlogram. (d) Peaked correlogram that is completely displayed in the output window. Vista velocity tracker display window. (e) Correlogram peaks are not fully displayed. (f) Two correlograms are centered.

Conversely, if the gain applied to the input signals is low, producing a flat correlogram with an ambiguous peak position [Fig. 2(c)], or high, such as to cause a saturation of the correlogram display [Fig. 2(a) and (b)], the velocity measurement will not be considered correct.

The Vista velocity tracker is based on the multiplication of the upstream signal that is delayed in a tapped digital delay line by the downstream signal using 64 hybrid analog–digital multipliers, placing each product on 64 fading memory circuits whose sequential readout generates the correlogram and maintains the maximum cross correlation that is spatially fixed at the 30-s by adjusting the system sampling frequency, which becomes directly proportional to the flow velocity. This process requires initial manual tuning of the frequency that controls the delay line to place the point of maximum correlation in the range of the feedback control that governs the system.

The measurements that are obtained with this system are strongly dependent on the operator skills since the detection of the correlation peak and, therefore, of the velocity is based on a visual understanding of the cross-correlogram display. The velocity measurement will be considered correct if two peaked correlograms are centered in the window display [Fig. 2(f)]; conversely, if the peaks are not centered and fully displayed in the window [Fig. 2(e)], the measurement will not be considered reliable. The automated frequency-tracking process is also strongly dependent on the initial velocity that is manually set by the operator.

III. Measurement System Implementation

The new analog–digital system for the measurement of blood flow velocity in microvessels is based on the conventional methods for dual-slit implementation through an electrooptic instrumentation (EOI) that yield upstream and downstream analog signals and uses a cross-correlation algorithm that is implemented with an innovative analog–digital cross correlator (AD-XCORR) that produces the velocity information.

An overview of the entire system is presented in Fig. 3.

The AD-XCORR consists of hardware devices that are controlled by software (e.g., MATLAB, xPC, RTW, and Visual C) that manages their communication and allows one to perform the analog-to-digital conversion of the analog signals through a National Instruments data acquisition (DAQ) board, calculates their cross correlation in real time on a dedicated microprocessor and random access memory, yields a visual output relative to the cross correlogram and velocity over time, and allows the tuning of parameters, making the system adjustable to the direction of the blood flow in the vessels and the microscope objective through a standard desktop personal computer.

A. EOI

The EOI consists of a conventional microscopic setup with customized optics integrated with photodiodes to convert the microscopic optic signals into the upstream and downstream analog signals, as shown in Fig. 1. A customized microscope is used to produce an image of a blood vessel in the optic plane containing the photodetector slits [20]. The target is visualized by transillumination using a 100-W mercury lamp. The physical size of the two slits is 0.6×2 mm; they are separated by 1.5 mm and located on the surface of a spherical field mirror along the axis of the magnified vessel image. The slits are used to define the areas of the field sensed by the optic sensors (photodiodes OPT301, 2.29×2.29 mm). The output of the photodiodes is passed through a 15-Hz low-pass filter and amplifiers (Tektronix 5A18N dual-trace amplifier).

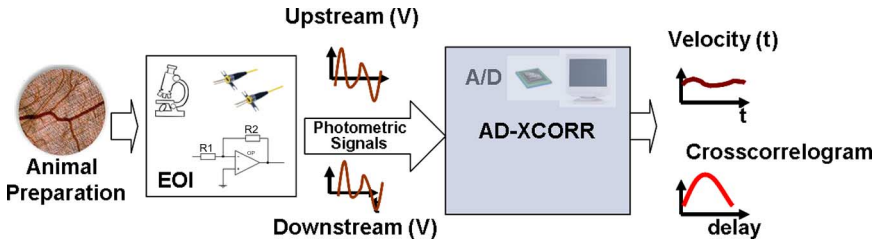

Fig. 3. Dual-slit-based velocity system. EOI that converts the changes in optical density due to the passage of RBCs into voltage signals (see Fig. 1).

A CCD camera (Panasonic industrial color CCD camera GP-KR222) is used to visualize on a monitor the target under observation. A beam divider mirror in the microscope axis directs the image to the eyepiece and the CCD camera. The image that is relayed to the viewing system is formed on the field mirror that contains the photometric slits, which are seen in their true position, sizes (w and h), and separation (SS) in the image that is projected by the microscope (see the vessel magnified image in Fig. 1). The real sizes of the slits on the microscopic image depend on the microscope magnification; the higher the magnification, the smaller the slits on the target. SS can be measured using a micrometer, whereas w and h can be calculated by dividing their physical sizes by the global magnification of the microscope (i.e., MM). Thus, in the case of objective magnification of $32\times$, the global magnification of the microscope due to the optics in between the objective and the outlet was calculated as $MM = 94$, which is the ratio between the physical separation between the slits and the one measured on the magnified image. The width of the slits in this case can therefore be calculated as $w = 0.6\ \text{mm}/94 = 6.4\ \mu\text{m}$. Such spatial resolution is flexible and can be improved using a microscope objective with higher magnification.

B. Cross-Correlation Algorithm

The cross-correlation function is exploited for time-delay estimation between signals for several applications in signal theory and analysis [21]. In the cross-correlation method, the time delay is estimated by searching for the maximum correlation coefficient between two signals, which, in this case, are relative to the same phenomena (transition of RBCs) but delayed with respect to each other. In the continuous-time domain, (1) represents the cross-correlation function. It is a function of the delay τ between the upstream (Up) and downstream (Dn) signals ranging in the infinite continuous-time domain, i.e.,

$$C_{\text{UpDn}}(\tau) = \lim_{a\to\infty} \frac{1}{a} \int_{-a/2}^{a/2} \text{Up}(t-\tau)\text{Dn}(t)dt. \quad (1)$$

It can be approximated in the discrete-time representation and adapted to computational implementation by

$$C_{\text{UpDn}}(hT_s, nT_s) = \sum_{k=0}^{M} \text{Up}\left[(h-k)T_s - nT_s\right] \text{Dn}\left[(h-k)T_s\right]$$
$$n = \{1, 2, 3, \ldots, n_{\max}\}. \quad (2)$$

C_{UpDn} represents the cross correlation that is calculated at the generic instant hT_s as a function of the delay between the two signals nT_s. The parameter M is the number of samples of the limited integration time window, n is the delay samples between the two signals, T_s is the sampling period, and $n_{\max} * T_s$ is the maximum detectable delay $d_{\max}$.

A time record of the upstream signal with length $d_{\max} = n_{\max} * T_s$ is dynamically stored in a circular vector $(1 \times n_{\max})$. At the time hT_s, new samples of the signals $(\text{Up}(hT_s), \text{Dn}(hT_s))$ are acquired. The upstream vector is updated by replacing the oldest value $(\text{Up}[(h - n_{\max} - 1)T_s])$ with the new one. $\text{Dn}(hT_s)$ is multiplied by each of the stored upstream samples $(\text{Up}(hT_s - nT_s) * \text{Dn}(hT_s))$, and the results vector $(1 \times n_{\max})$ is loaded in an integrator as a row of a circular matrix $(M \times n_{\max})$, replacing the row related to the oldest multiplication at the instant $(h - M - 1)T_s$, which can be considered irrelevant for the calculation of the correlation. The integration is performed by sums of each column elements, which corresponds to an element of the cross-correlogram vector $(C_{\text{UpDn}}(nT_s))$.

The system detects the maximum of the correlation curve and computes the velocity of blood for every acquired sample. Consequently, the system reaches the best possible resolution of the velocity curve in the time domain.

A code optimization policy was exploited to make this algorithm computationally light and unaffected by the integration time $(M * T_s)$ and, therefore, recursive [22] since elaboration can be performed within a sampling period. It requires large memory allocation to store the upstream time window and, above all, to allocate the integration matrix.

IV. Results and Discussion

A theoretical analysis of the uncertainty in the implemented algorithm was carried out to test the reliability of the system. The system was also tested during *in vitro* and *in vivo* experiments.

In vitro tests were performed for system calibration and parametric characterization. In particular, we carried out a study to determine the system sensitivity to changes of parameters, such as gain amplification, which is applied to the voltage input signals.

In all the studies and experiments, the sampling rate for DAQ, analog-to-digital conversion, and execution of the cross-correlation task was fixed at $F_S = 5$ kHz. It was considered to be a good compromise for uncertainty, resolution matters (see Section IV-A and B, respectively), and execution time considerations.

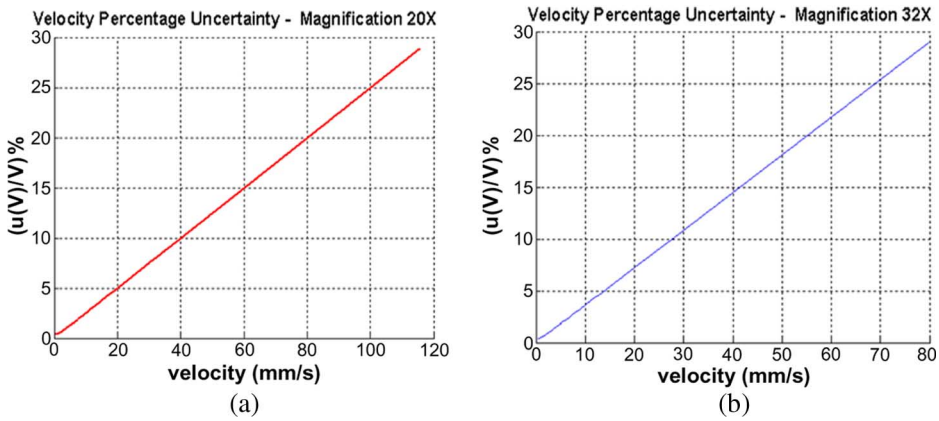

Fig. 4. (a) Relative uncertainty for magnification of 20×. (b) Relative uncertainty for magnification of 32×.

A. *Uncertainty Analysis*

A theoretical study of the combined uncertainty of the velocity measurement $u_c(v)$ was performed for two different optical magnifications with two microscope objectives (useful magnification (UM) 20× and UM32×) to determine the reliability of the developed system.

According to the velocity–delay relationship of the dual-slit methodology, the velocity v is a function of SS, whereas the detected delay d is a function of $v = SS/d$, and therefore, considerations on the propagation of uncertainty [23] indicate that the total probable uncertainty $u_c(\nu)$ can be considered as a function of the uncertainty $u(SS)$ and the average value of SS, which was obtained through multiple measurements using a micrometer. The uncertainty in the delay detection $u(d)$ is mainly due to the time resolution of the system that is determined by the sampling period $T_s = 200$ μs, and it can be calculated by assuming a uniform distribution of probability.

The evaluation of the slit separation was experimentally performed using the micrometer to perform ten measurements for each magnification (20× and 32×).

The slit separation mean value SS_M and the standard deviation SD, which, in this case, is equivalent to the uncertainty $u(SS)$, were calculated, and the following values were obtained: $SS_M = 15.9$ μm and $u(SS) = SD = 5.7 * 10^{-2}$ μm for magnification of 20×, and $SS_M = 23.1$ μm and $u(SS) = SD = 8.3 * 10^{-2}$ μm for magnification of 32×. The micrometer measurement is very accurate, and therefore, the SS measurement contribution to the combined uncertainty is considered negligible.

The uncertainty relationship can therefore be simplified to (3), where u_c is expressed as a function of the mean value of velocity for each measurement point, i.e.,

$$u_c(v_M) = \sqrt{\left(\frac{\partial v}{\partial d}\right)^2_M u(d)^2} = \left|\left(\frac{\partial v}{\partial d}\right)_M u(d)\right| = \frac{SS_M}{d_M^2}u(d) = \frac{v_M^2}{SS_M}u(d). \quad (3)$$

Here, a study of the relative percentage uncertainty is considered basic since most of the microcirculation analyses are based on a comparison between a control state and the state under study. Percentage changes in velocity between the two conditions are, in fact, of interest and are affected by the measurement system.

Curves of the percentage relative error $((u_c(v_M)/v_M) * 100)$ for both magnifications of 20× and 32× were obtained using (3) for a range of measurement points of velocity (considering the mean value for each measure), including the values determined in *in vivo* experimentation on small animals, as shown in Fig. 4(a) and (b). The curves show, as expected, a linear trend as a function of velocity since the uncertainty increases as the measured velocity increases, and this is due to the inverse proportionality between the velocity and the delay, which is directly measured by the system.

In the range of expected velocities in *in vivo* experiments in small animals (rats and hamsters, 0.5–20 mm/s), the maximum percentage uncertainties are 6% and 8% at 25 mm/s for magnifications of 20× and 32×, respectively, and these values decrease by about 0.4% at 0.5 mm/s for both magnifications.

B. *System Calibration*

Calibration of the system was performed with two microscope objectives (UM20× and UM32×). A rotating semitransparent wheel with adjustable velocity and with its surface textured to simulate the blood vessel image was used as a test target.

The wheel was placed under the microscope, and the photodiodes that were oriented along the direction of motion of the pattern provide the signals for processing by the newly developed AD-XCORR. The linear velocity of the wheel was calculated using the known distance between the center of the wheel and the area under the microscope objective, and the revolution time of the wheel was measured with a chronograph.

The delay time between the upstream and downstream signals was detected using the developed AD-XCORR.

Calibration curves were obtained by plotting the *in vitro* velocity experimental results versus the detected delay. An example of a calibration curve relative to the UM20× magnification is shown in Fig. 5.

The experimental velocity values (dotted line with crossed marks) were compared with the velocity value curves that were obtained using the hyperbolic velocity–delay relationship (solid

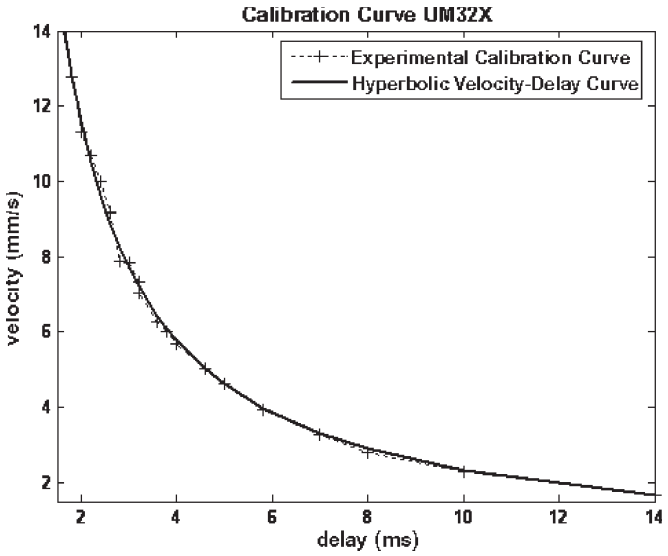

Fig. 5. Calibration curve with the microscope objective UM32×: Experimental curve (dotted line with crossed marks) and hyperbolic velocity–delay relationship (solid line).

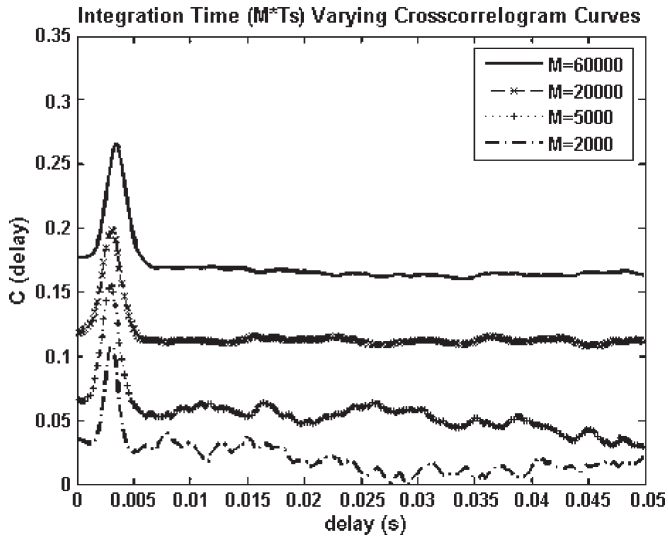

Fig. 6. Cross correlogram at variable integration times (UM20×).

line), which is given by $v = SS_M/d$. The delay was measured by the new developed cross correlator.

The theoretical velocity functions that were calculated using the mean measured SS for the two microscope magnifications are given by $v_{20\times} = (23.1E-6)/d$ and $v_{32\times} = (15.9E-6)/d$. Conversely, the obtained curves through the experimental calibration are $(v_{20\times})_{\exp} = (22.1E-6)/d^{1.007}$ with a squared correlation coefficient of $R^2 = 0.9986$ and $(v_{32\times})_{\exp} = (14.88E-6)/d^{1.012}$ with $R^2 = 0.995$. The squared correlation coefficient value that is close to the unit allows one to assess that the experimental curves are a very good approximation of the hyperbolic curves.

The velocity ranges that can be measured are 0.3–75 mm/s (UM32×) and 0.48–120 mm/s (UM20×) for $d_{\max} = n_{\max} * T_s = 50$ ms.

C. System Sensitivity to the Parameter Changes

In the implementation of the cross-correlation algorithm according to the function in (2), the choice of parameters such as $n_{\max}$, T_s, and M is related to the physiological phenomenon dynamics and the EOI setup.

The maximum delay $d_{\max} = n_{\max} * T_s$, which affects the performance of the system and the cross-correlation task execution time, was chosen for the measurement of the minimum expected velocity and the time that is necessary to perform the algorithm computation.

The sampling period T_s depends on the frequency spectrum of the upstream and downstream signals, but it is also chosen by considering the uncertainty, the velocity range, and the time slot that are devoted to the algorithm execution. It thus affects the minimum detectable delay $(n = 1)$ between the two input signals and, therefore, the resolution in the velocity measurement and $u(d)$. A compromise between the required resolution and the performance of the algorithm computations was considered at $T_s = 200$ μs.

The integration time $M * T_s$ affects noise rejection and the dynamic response of the system. A detailed parametric study has been carried out by letting $M * T_s$ be variable and maintaining the calibration velocity and T_s fixed.

Fig. 6 shows the cross correlogram for the different values of the integration time in the range from 40 ms $(M = 2000)$ to 12 s $(M = 60\,000)$ using the UM20× microscope objective.

For long integration times, the cross correlogram has a smooth profile in the whole delay range, and for short periods of $M * T_s$, the cross correlogram presents irregularity after the maximum. This is due to the noise filtering performed by the integration factor; on the other hand, it makes the system more robust to random events, i.e., animal movements, and to systematic disturbance, i.e., EOI system pathway.

Increasing the integration time also increases the cross-correlogram offset because more information is accumulated over time. Long integration times provide good noise rejection; however, a large value of M affects the dynamic response of the system.

Finally, another important parameter that affects the performance of the system is the gain amplification that is applied to the voltage signals acquired by the photodiodes, which affects the signal-to-noise ratio in the outcome of the cross-correlation algorithm. This factor was analyzed using a UM20× microscope objective, maintaining the rotation velocity of the wheel constant, using a fixed integration time of $M * T_s = 2$ s $(M = 10\,000)$, and varying the gain of the amplifiers.

Fig. 7(a) shows how the peak amplitude in the cross correlogram proportionally varies as a function of the signal gain G for $G = 100,\ 200,\ 500,\ 2000,$ and $10\,000$. The amplified signal dynamics with respect to the analog-to-digital input range (−10 V/10 V) never reaches the saturation level. It is proved by the shape of the cross-correlation curve, which is smooth and peaked, and therefore does not present the typical flat trend of saturated curves [see the example of the saturated cross correlogram in Fig. 2(a) and (b)].

The limiting case for the hybrid AD-XCORR occurs at the lowest gain (see Fig. 7(b); $G = 2$) when the cross correlogram

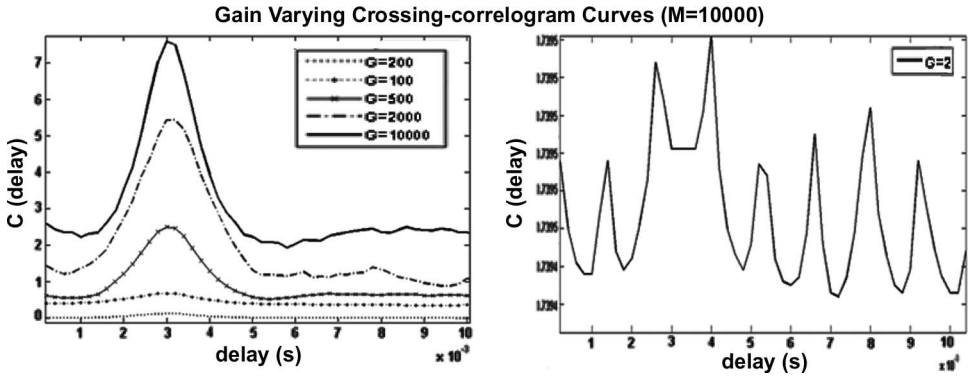

Fig. 7. (a) Cross-correlation curves with the varying gain of the input signals. (b) Details of the cross-correlation curves for a low gain.

loses its peaked shape, because, for low gains, the noise amplitude is comparable to the amplitude of the meaningful signals.

In conclusion, the advantage of the new hybrid system as compared with the conventional existing cross correlators is that a high gain in the amplification of the signals can be used to have a more peaked cross correlogram with no saturation effects, which provides improved detection of maximum cross correlation. The AD-XCORR relies on wide hardware–software resources, which allow a considerable amount of data to be stored and a wide range of velocities to be measured with a good resolution.

D. System Testing in Experimental Conditions

In vivo experiments were carried out in the rat cremaster muscle preparation since it offers an extensible, transparent, and thin skin layer, avoiding overlapping of vessels and, therefore, optical interferences.

Sprague–Dawley rats were anesthetized with an intraperitoneal injection of 50 mg/kg pentobarbital sodium (Abbott). Additional anesthetic was administered throughout the experiment as needed. The carotid artery was catheterized for blood withdrawals and pressure measurements, and the jugular vein was catheterized for administration of anesthetic. The arterial catheter was filled with a solution of heparinized saline to prevent clotting. The rat cremaster muscle was placed on a stage and prepared for intravital microscopy [24]. The animal was then placed on a Plexiglas platform with a raised area, which enabled viewing of the muscle while maintaining normal blood flow. The muscle was suffused with Plasma-Lyte A and covered with a thin polyvinyl film. A temperature probe was placed beside the muscle to maintain the temperature at 37 °C throughout the experiment [25]. The animal studies were approved by the Animal Subjects Committee, University of California, San Diego (UCSD).

Characterization of blood flow velocity consisted in measuring the average values, and test of the dynamic response of the system was determined from continuous records using a UM20× microscope objective.

To perform the comparison of a newly developed system with a conventional method, a statistically significant number of velocity measurement was performed. The vessels were chosen by a skilled operator on the skin surface, in good light and skin conditions for transillumination, avoiding skin layers with pathological conditions, which makes the measurement difficult (causing the vessel image to be blurred), and considering the depth of the vessels, which is equal to their diameter. Blood flow velocity was measured in vessels with the diameter in the range of 10–100 μm, resulting in 184 different velocity measurements that are simultaneously performed with the new AD-XCORR system and with the HP digital cross correlator (available in the Microhemodynamic Laboratory, UCSD), in the range between 0 and 25 mm/s.

The standard deviation of the error between the two performed measurements is 0.7% with respect to the full scale of the system. This indicates that both systems provide consistent results.

In addition, to study the dynamic behavior of the developed system, a 35-μm-diameter arteriole that was subjected to a hypoxic episode was observed for 8 min. The animal was observed for 2 min under normal conditions. Then, the animal was made to inspire 7% oxygen for 1 min and then was observed until its condition returned to normal.

The integration time of the AD-XCORR was set at 3 s as a good tradeoff between the dynamic response and noise filtering. A continuous record was obtained as the voltage output from the AD-XCORR system and was acquired in real time by the Biopac hardware. The blood pressure of the animal was simultaneously recorded.

The red trace in Fig. 8 (top) is the blood pressure (in millimeters mercury), and the green trace in Fig. 8 (bottom) is the velocity record (in centimeters per second). A drop in blood pressure coincides with a drop in blood flow velocity.

The AD-XCORR calculates and shows in real time to the operator the cross correlogram during the whole experiment. The continuous visualization of the cross correlogram during the experiment insures that the velocity measurement is reliable. An example of the cross correlogram is shown in Fig. 9; it presents the typical shape of the correlation curve by assessing the correctness of the velocity reading in the considered experiment.

V. Conclusion

A real-time noninvasive measurement system for the automatic, continuous, and real-time measurement of blood flow velocity in the microcirculation was developed.

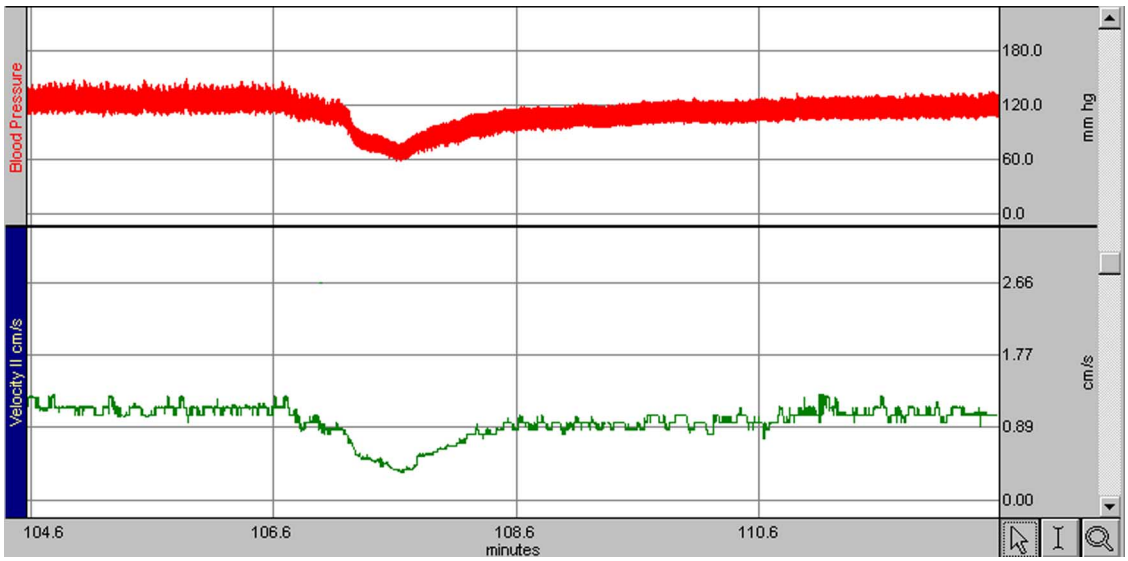

Fig. 8. Hypoxia experiment and monitoring of a 40-μm arteriole. Top: Blood pressure reading (in millimeters mercury). Bottom: AD-XCORR velocity reading (in centimeters per second).

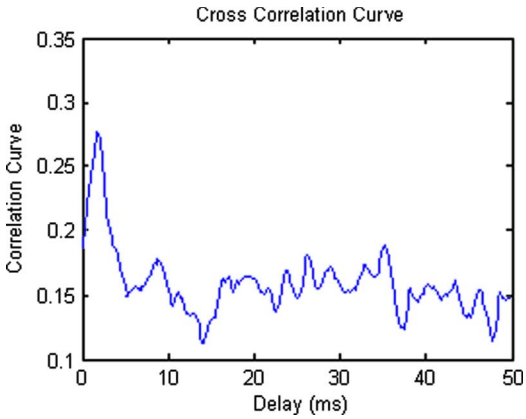

Fig. 9. AD-XCORR cross correlogram during the hypoxia experiment. It presents the typical shape of the correlation curve by assessing the correctness of the velocity reading in the hypoxia experiment.

It has been implemented using a system based on a conventional dual-slit velocimetry, where the data are processed using a hybrid analog–digital approach, implemented by an AD-XCORR. The new system exploits hardware–software resources, implementing an optimized recursive cross-correlation function through a software algorithm in a real-time environment.

The calibration of the system, the parametric studies, and the theoretical calculation of the measurement uncertainty were performed using a known velocity target. These characterizations allowed one to determine the detectable velocity range (0.3–120 mm/s), to determine the relative uncertainty on the measurement, and to assess the sensitivity of the system to critical parameters such as the gain applied to the analog input signal and the integration time in the cross-correlation algorithm.

A statistically meaningful number of *in vivo* measurements were performed to test this system and to show that the results are consistent with the ones obtained by the conventional analog cross correlator.

Moreover, the dynamic response of the AD-XCORR was tested during a real case study, as represented by a hypoxia experiment. The detected velocity changes were consistent with the physiological response of the animal.

The AD-XCORR overcomes some drawbacks of the conventional analog measurement systems. It allows a wide range of velocity readings during the same experiment without changing any of the system parameters. It makes the measurement independent from hardware tolerances. Moreover, system automation makes measurements independent from the user experience and void of operator-related biases.

The system presents flexibility in relation to the various experimental working conditions; it can give average velocity values and continuous readings and provides a method for recording results and tuning parameters and a user-friendly interface. The optimization of the implementation in terms of memory allocation and execution time makes the system portable and scalable to different technologies, yielding to more compact solutions. Further studies in the direction of the electrooptical system implementation can also be carried out to allow the integration of more flexible sensing and processing systems for more complex and distributed analysis of the microfluidic phenomena and systems.

REFERENCES

[1] H. G. Klein, "Oxygen carriers and transfusion medicine," *Int. J. Artif. Cells Blood Substit. Immobil. Biotechnol.*, vol. 22, no. 2, pp. 123–135, 1994.

[2] J. C. Bowersox and J. R. Hess, "Trauma and military applications of blood substitutes," *Int. J. Artif. Cells Blood Substit. Immobil. Biotechnol.*, vol. 22, no. 2, pp. 145–159, 1994.

[3] M. Intaglietta, *Microcirculatory Basis for the Design of Artificial Blood*. New York: Stockton, 1999.

[4] P. Zhong, Y. Zhou, and S. Zhu, "Dynamics of bubble oscillation in constrained media and mechanisms of vessel rupture in SWL," *Ultrasound Med. Biol.*, vol. 27, no. 1, pp. 119–134, Jan. 2001.

[5] J. R. Lindner, S. Ismail, W. D. Spotnitz, D. M. Skyba, A. R. Jayaweera, and S. Kaul, "Albumin microbubble persistence during myocardial contrast echocardiography is associated with microvascular endothelial glycocalyx damage," *Circulation*, vol. 98, no. 20, pp. 2187–2194, Nov. 1998.

[6] A. Bouakaz, M. Versluis, and N. De Jong, "High-speed optical observations of contrast agent destruction," *Ultrasound Med. Biol.*, vol. 31, no. 3, pp. 391–399, 2005.

[7] C. T. Chien and P. N. Burns, "Investigation of the effects of microbubble shell disruption on population scattering and implications for modeling contrast agent behavior," *IEEE Trans. Ultrason., Ferroelectr., Freq. Control*, vol. 51, no. 3, pp. 286–292, Mar. 2004.
[8] C. K. Holland, C. X. Deng, R. E. Apfel, J. L. Alderman, L. A. Fernandez, and K. J. Taylor, "Direct evidence of cavitation *in vivo* from diagnostic ultrasound," *Ultrasound Med. Biol.*, vol. 22, no. 7, pp. 917–925, 1996.
[9] J. L. Borders and H. J. Granger, "An optical Doppler intravital velocimeter," *Microvasc. Res.*, vol. 27, no. 1, pp. 117–127, Jan. 1984.
[10] H. Cohen and D. Marsh, "Vitro calibration of a video-based method for measuring blood velocity in kidney medulla and other tissues subject to respiratory motion," *Microvasc. Res.*, vol. 19, no. 3, pp. 277–287, May 1998.
[11] M. Linden, H. Golster, S. Bertuglia, A. Colantuoni, F. Sjoberg, and G. Nilsson, "Evaluation of enhanced high-resolution laser Doppler imaging in an *in vitro* tube model with the aim of assessing blood flow in separate microvessels," *Microvasc. Res.*, vol. 56, no. 3, pp. 261–270, Nov. 1998.
[12] H. Golster, M. Linden, S. Bertuglia, A. Colantuoni, G. Nilsson, and F. Sjoberg, "Red blood cell velocity and volumetric flow assessment by enhanced high-resolution laser Doppler imaging in separate vessels of the hamster cheek pouch microcirculation," *Microvasc. Res.*, vol. 58, no. 1, pp. 62–73, Jul. 1999.
[13] K. Wardell and G. E. Nilsson, "Duplex laser Doppler perfusion imaging," *Microvasc. Res.*, vol. 52, no. 2, pp. 171–182, Sep. 1996.
[14] K. Tsukada, H. Minamitani, E. Sekizuka, and C. Oshio, "Image correlation method for measuring blood flow velocity in microcirculation: Correlation 'window' simulation and *in vivo* image analysis," *Physiol. Meas.*, vol. 21, no. 4, pp. 459–471, 2000.
[15] Y. Sugii, S. Nishio, and K. Okamoto, "*In vivo* PIV measurement of red blood cell velocity field in microvessels considering mesentery motion," *Physiol. Meas.*, vol. 23, no. 2, pp. 403–416, May 2002.
[16] H. Wayland and P. C. Johnson, "Erythrocyte velocity measurement in microvessels by a two-slit photometric method," *J. Appl. Physiol.*, vol. 22, no. 2, pp. 333–337, Feb. 1967.
[17] B. Zimmerhackl, J. Tinsman, R. L. Jameon, and C. R. Robertsons, "Use of digital cross-correlation for on-line determination of single-vessel blood flow in the mammalian kidney," *Microvasc. Res.*, vol. 30, no. 1, pp. 63–74, 1985.
[18] N. R. Silvermann, M. Intaglietta, and W. R. Tompkins, "A video densitometer for blood flow measurement," *Brit. J. Radiol.*, vol. 46, pp. 594–598, 1973.
[19] M. Intaglietta, G. A. Breit, and W. R. Tompkins, "Four window differential capillary velocimetry," *Microvasc. Res.*, vol. 40, no. 1, pp. 46–54, Jul. 1990.
[20] J. H. Holcomb, "A new instrument for measurement of microcirculation dynamics in living tissue," M.S. thesis, Univ. Arizona, Tucson, AZ, 1978.
[21] G. Jacovitti and G. Scarano, "Discrete time techniques for time delay estimation," *IEEE Trans. Signal Process.*, vol. 41, no. 2, pp. 225–233, Feb. 1993.
[22] F. Sapuppo, D. Longo, M. Bucolo, M. Intaglietta, L. Fortuna, and P. Arena, "Real-time blood flow velocity monitoring in the microcirculation," in *Proc. 26th Annu. Int. Conf. IEEE EMBC*, San Francisco, CA, Sep. 2004, pp. 2219–2222.
[23] *ISO—Guide to the Expression of Uncertainty in Measurement*, 1997.
[24] G. L. Anderson, R. D. Acland, M. Siemionow, and S. J. McCabe, "Vascular isolation of the rat cremaster muscle," *Microvasc. Res.*, vol. 36, no. 1, pp. 56–63, Jul. 1988.
[25] J. J. Bishop, P. R. Nance, A. S. Popel, M. Intaglietta, and P. C. Johnson, "Relationship between erythrocyte aggregate size and flow rate in skeletal muscle venules," *Amer. J. Physiol. Heart Circ. Physiol.*, vol. 286, no. 1, pp. H113–H120, Jan. 2004.

Francesca Sapuppo (S'00) received the M.S. degree in microelectronics engineering and the Ph.D. degree in electronic and control engineering from the University of Catania, Catania, Italy, in 2003 and 2007, respectively.

She currently holds a postdoctoral position with the University of Catania, carrying out research in the field of biomicrofluidic control engineering and working on electrooptical instrumentation, image processing, and cellular neural networks for real-time monitoring systems, distributed control of microfluidic processes, and nonlinear data analysis applied to biological phenomena.

Maide Bucolo (S'99–M'01) received the computer science engineering degree and the Ph.D. degree in electronic and control engineering from the University of Catania, Catania, Italy, in 1997 and 2001, respectively.

She is currently an Assistant Professor with the University of Catania. Moreover, she has been involved in several projects that are supported by public institutions and a consortium of private companies. Her research activity mainly involves the study of complex dynamics, cellular neural networks, and nonlinear time series analysis for biomedical applications.

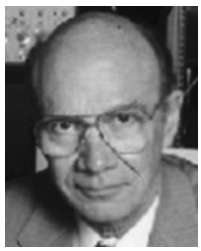

Marcos Intaglietta received the M.S. and Ph.D. degrees in applied mechanics from the California Institute of Technology, Pasadena, in 1959 and 1963, respectively.

He is currently a Professor of bioengineering with the University of California, San Diego, La Jolla, where he directs the Microhemodynamic Laboratory, specializing in the analysis of transport phenomena in the microcirculation and the development of blood substitutes.

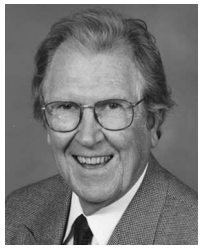

Paul C. Johnson received the B.S. degree in physics and the Ph.D. degree in physiology from the University of Michigan, Ann Arbor.

He did his postdoctoral work at Case Western Reserve University, Cleveland, OH. Subsequently, he taught at Indiana University, Bloomington, and the University of Arizona, Tucson, and is currently an Adjunct Professor of bioengineering with the University of California, San Diego, La Jolla. His research interest is on the microcirculation and mechanisms of blood flow regulation, particularly the active response of the arterioles to intravascular pressure (i.e., myogenic response). More recently, his research has emphasized the contributions of *in vivo* blood rheology to the microcirculatory function.

Dr. Johnson was a recipient of a number of honors and awards for his research, including the Eugene M. Landis Award of the Microcirculatory Society, the Carl J. Wiggers Award of the American Physiological Society, and the Doctor of Medicine Honoris Causa from Maastricht University, Maastricht, The Netherlands.

Luigi Fortuna (M'90–SM'99–F'00) received the Bachelor's degree in electrical engineering from the University of Catania, Catania, Italy, in 1977.

He was a Researcher in electronics with the University of Catania until 1987, when he became an Associate Professor of automatic control. He has been a Full Professor of system theory since 1994 and is currently the Dean of the School of Engineering, University of Catania. He has coordinated research projects that are supported by public institutions and a consortium of private companies. He is a coauthor of six books, among which is *Cellular Neural Networks* (Springer, 1999). He is the holder of several U.S. patents. His scientific interests include nonlinear science and complexity, chaos, and cellular neural networks, with applications in bioengineering.

Paolo Arena (S'93–M'97–SM'01) received the M.S. degree in electronic engineering and the Ph.D. degree in electrical engineering from the University of Catania, Catania, Italy, in 1990 and 1994, respectively.

He is currently an Associate Professor of system theory with the University of Catania. His research interests include adaptive and learning systems, neural networks, cellular neural networks, and collective behavior in living and artificial neural structures, bioimage analysis, and DNA microarrays.